

Comparative Study of Iron and Trace Element Mobilization during Fe-Oxide Bioreduction in Mine Tailings: a case study of Ensenada Chapaco (Chile) and Portman Bay (Spain)

Robert Benaiges-Fernández^{1,2*} Jordi Palau³ Jordi Urmeneta^{2,4} Jordi Cama¹ Josep M. Soler¹ Bernhard Dold^{5,6}

¹Institute of Environmental Assessment and Water Research (IDAEA), CSIC, Barcelona
08034, Catalonia, Spain. E-mail Robert Benaiges-Fernández: robertbenaiges@gmail.com

²Department of Genetics, Microbiology and Statistics, University of Barcelona
Barcelona 08028, Catalonia, Spain

³Department of Mineralogy, Petrology and Applied Geology, Faculty of Earth Sciences, University of Barcelona
Barcelona 08028, Catalonia, Spain

⁴Biodiversity Research Institute (IRBio)
Barcelona 08028, Catalonia, Spain

⁵Sustainable Mining Research and Consultancy (SUMIRCO)
San Pedro de la Paz, Chile

⁶Pontifical Catholic University of Peru (PUCP)
Lima, Peru

ABSTRACT

Bioreduction of Fe-oxides in mine tailings deposited under marine conditions releases Fe and associated trace elements (*e.g.* Ti, Ni, Cd, Pb), leading to contamination of the marine environment. Sea-Tailings Disposal (STD) along the northern coast of Chile (Ensenada Chapaco) and along the eastern coast of Spain (Portman Bay) results in an adverse impact on the environment. This paper focuses on bioreduction under marine conditions. To this end, two column experiments were carried out with samples from Portman Bay and Ensenada Chapaco. Lactate (*i.e.* organic matter source) was supplied during the experiments. The results obtained are compared with those from batch experiments performed under similar conditions.

In the column filled with Portman Bay tailings, the high content of magnetite (15wt%) in contact with water gives rise to a large magnetite surface area and abundant Fe(III), which results in a high release of Fe(II) and Trace Elements (TE). Since Fe(II) adsorbs onto the magnetite surface reducing the availability of Fe(III), the magnetite bioreduction and the consequent TE release decrease after 2000h. By contrast, the magnetite bioreduction lasts longer (3000h) in the column with Ensenada Chapaco tailings. This is because a lower magnetite content in the tailings (1wt%) provides a smaller reactive surface area yielding less Fe(III). Consequently, the concentrations of Fe(II) and TE in the output solutions are lower, which slows down the Fe(II) adsorption onto magnetite. This results in a longer magnetite bioreduction. Bioreduction is regulated by the availability of Fe(III) in both columns.

It is inferred that the bioreduction rate diminishes as a function of time and increases as a function of soluble Fe(II) concentration. Moreover, the concentrations of TE released from the two bioreduced tailings exceed the elemental concentrations under marine conditions.

KEYWORDS | Oxide reduction. Sea tailings deposition. Marine pollution. Mine waste. Magnetite.

INTRODUCTION

The discharge of mining waste into the sea (Sea-Tailings Disposal; STD) poses a serious risk to the environment. In the early 20th century the flotation process revolutionized mining, making it possible to exploit low-grade ores (Dold, 2014). This led to a considerable increase in the volume of tailings. STD has been practiced only by a small number of mines (Vare *et al.*, 2018). For instance, in 2015, only 16 of the current 2500 large industrialized mines worldwide utilized STD (“Proceeding of the GESAMP International Workshop on the Impacts of Mine Tailings in the Marine Environment | GESAMP,” n.d.). This included mines in Norway such as Sørfjord mine (Cu, Pb, Zn), Papua New Guinea’s Lihir island mine (Au), Simberi island mine (Au), Ok Tedi mine (Au, Cu) and in Chile Los Colorados mine (Fe) (Koski, 2012). Today, large active mines in Norway (*i.e.*, Rana Gruber mine) continue using STD (Jensen *et al.*, 2019; Ramirez-Llodra *et al.*, n.d.). However, between 15 and 20 mines are considering STD as a future disposal option (Davies *et al.*, n.d.). The international legislative framework for STD, comprising the London Convention (1972) and the London Protocol (1996), prohibits the dumping of waste into the sea (Dold, 2014). An exception is made for “inert, inorganic geological material,” under which tailings may be classified (Kwong *et al.*, 2019; Medina *et al.*, 2005).

The environmental impact of STD is a significant global concern, leading to the accumulation of toxic heavy metals (*e.g.* cadmium, lead, and nickel) and the disruption of marine ecosystems (Simonsen *et al.*, 2019). These contaminants not only pose hazards to marine life but also enter the food chain, ultimately affecting human health. Previous studies have shown that cadmium, lead and nickel accumulate in marine organisms, leading to long-term ecological imbalance (dos Santos *et al.*, 2014). Despite its serious environmental implications, STD remains a common waste-management practice in some regions, highlighting the need for a thorough investigation into its environmental impacts (Ramirez-Llodra *et al.*, 2015).

Portman Bay (La Unión, Spain) operating between 1958 and 1991 and Ensenada Chapaco (Huasco, Chile) operating between 1978 and 2018 are two prominent examples with extensive STD. They have been selected because for their history of contamination and their potential for research. Metal contamination of sea water due to STD has been previously described at Chañaral Bay (North of Chile) (Medina *et al.*, 2005; technology and 2006, 2006) and at Portman Bay (Manteca *et al.*, 2014a) (Fig. 1).

Portman Bay (37°35′02.3″N 0°50′55.4″W) is located in the municipality of La Unión (Murcia, SE Spain). Given its proximity to the Sierra de Cartagena-La Unión mining district, an ore concentration facility was opened along the

bayside (Lavadero Roberto) to treat complex ores from the mining deposits (Peña *et al.*, n.d.). Between 1958 and 1991 this plant discharged approximately 60Mt of tailings into the sea leaving behind knippazardous waste (metal-rich) artificial soils that brought forward the shoreline about 500-600m. This was the worst case of contamination due to mining waste in the western Mediterranean, contributing 50% of the heavy metal input and around 90% of the solid waste input to the Mediterranean Sea (Autónoma De Baja *et al.*, 2008). At present, more than 80% of Portman Bay is filled with tailings (Benavente *et al.*, 2020).

Ensenada Chapaco (28°29′03.1″S 71°15′52.6″W) is in the municipality of Huasco (Atacama, Chile). An iron oxide pellet plant is located along the bay that is contaminated by mining waste mainly from the Los Colorados, El Algarrobo and Los Cristales mines, known Iron Oxide-Apatite (IOA) mineral deposit (Knipping *et al.*, n.d.; Sillitoe, 2003). Mining activity commenced in 1978 and ceased in 2018. The plant generated up to 4t of tailings daily, which were discharged 500m offshore into the sea. Previous studies had evaluated the impact of 16years of tailings disposal on the macro benthic community in the intertidal zone (1978–1994; (Autónoma De Baja *et al.*, 2008; Benavente *et al.*, 2020; Vare *et al.*, 2018). Prolonged disposal of mine tailings on the sea bed had caused substantial damage to the profusion and diversity of marine species (González *et al.*, n.d.; Lancellotti *et al.*, n.d.).

To fully understand the environmental consequences of STD, it is essential to quantify the chemical evolution of materials disposed under marine conditions. This implies the provision of parameters associated with changes in metal concentration, microbial activity and sediment chemistry (Chen *et al.*, 2016), providing critical insights into the fate of the contaminants. The biogeochemical behavior of iron (Fe) and Trace Elements (TE) in the tailings determines the environmental impact on marine ecosystems. Fe and TE influence the mobilization of associated contaminants, increasing the bioavailability of toxic metals in these ecosystems (Palau *et al.*, 2021). Fe(III) bioreduction, that is driven by Dissimilatory Iron-Reducing Bacteria (DIRB), is a key process that influences the release of trace metals (Zachara *et al.*, 2001). The bacterial activity can transform less soluble iron phases into more soluble forms, potentially mobilizing associated trace elements (*e.g.* lead and cadmium) into the marine environment (Esther *et al.*, 2015). Earlier studies by Lovley *et al.* (1986) (Lovley and Phillips, 1986) and Lonergan *et al.* (1996) (Lonergan *et al.*, 1996) demonstrated the widespread occurrence of Fe(III)-reducing bacteria in marine sediments and their significant role in biogeochemical cycles. Given the role of these bacteria, Fe(III) bioreduction should be studied to evaluate the impact of STD.

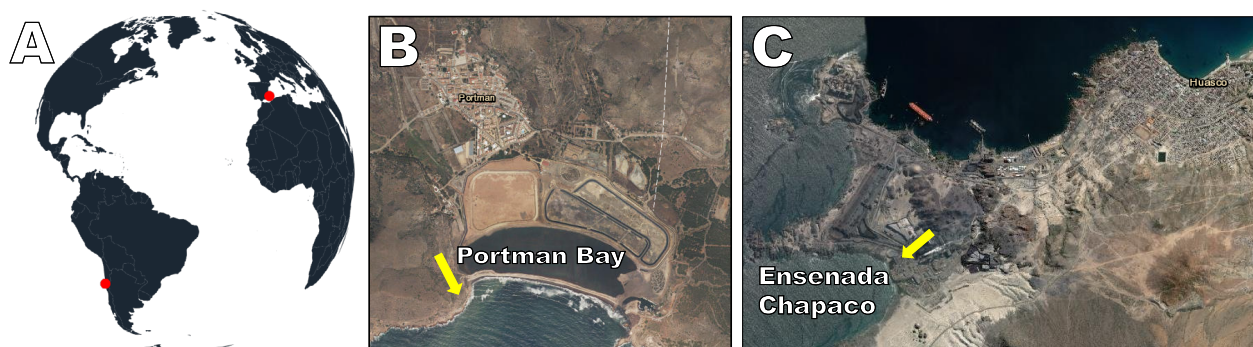


FIGURE 1. Studied mine disposal sites. A) Location of Portman Bay in La Unión, on the southern Iberian Peninsula, and of Ensenada Chapaco in Huasco, northern Chile. B) Aerial photograph of Portman Bay full of tailings. C) Aerial photograph of Ensenada Chapaco and the location of an iron oxide pellet plant. Yellow arrows indicate the location of the tailings disposal pipes (González *et al.*, n.d.; Manteca *et al.*, 2014b). Satellite images obtained from <https://earthexplorer.usgs.gov>.

As a result of oxygen depletion by microbial activity in STD-marine sediments, Fe- and Mn-oxides are subject to bioreduction (Benaiges-Fernandez *et al.*, 2019). It plays a crucial role in the mobilization of associated contaminants, which can have significant ecological implications (Palau *et al.*, 2021). Given the extensive contamination history of Portman Bay and Ensenada Chapaco, these cases present ideal conditions for studying the processes and mechanisms of metal mobilization (Alorda-Kleinglass *et al.*, 2019).

The environmental impact of tailings disposal is linked to the microbial processes occurring in marine sediments. It is necessary to understand microbial processes to shed light on Fe and TE mobilization at these sites. This study aims to investigate the bioreduction of Fe and the release of associated TE at two well-characterized tailing sites (Portman Bay and Ensenada Chapaco). This provides insight into the underlying mechanisms of metal mobilization under marine conditions, which is decisive to i) predict the long-term fate of contaminants in STD-affected marine environments and ii) develop strategies to mitigate the environmental impact.

MATERIALS AND METHODS

Tailings characterization

The Portman Bay (PT) column was filled with tailings accumulated on the seashore. A representative sample was collected from the top 50cm of the tailings using a hand core sampler and immediately placed in sterile zip-lock plastic bags that were stored in the refrigerator at 4°C until use. The sample was subsequently ground and sieved to a size fraction between 60 and 100µm. Powder XRD-Rietveld analysis was used to obtain the mineralogical composition of the sample (Table 1). This

technique, known for its precision, has uncertainties of approximately ~0.5wt% for minor phases and 0.5–1.5wt% for major rock-forming minerals (Rahfeld *et al.*, 2018)

The Ensenada Chapaco (CT) column was filled with tailings from the iron oxide pellet plant in Huasco (Palau *et al.*, 2021). The tailings sample was obtained from the treatment plant and placed in a sterile zip-lock plastic bag to be stored at room temperature. Sample pore water was removed by centrifugation (3 times). The unsaturated sample was then sieved to obtain a size fraction between 60 and 100µm. Subsequently, powder XRD-Rietveld analysis was carried out to determine the mineralogical composition of the CT sample (Table 1).

To ensure sterilization, both tailings samples were autoclaved before filling the columns. Subsequent powder XRD analysis did not detect any new minerals.

TABLE 1. Mineral composition (wt%) of the Portman Bay (PT) and Ensenada Chapaco (CT) tailings used in the experiments

Mineral	Chapaco Tailings (CT)	Portman Tailings (PT)
Magnetite	1	15
Chlorite	22	
Hornblende	30	
Albite	28	
Hydrocalcite	3	
Talc	16	
Pyrite		37
Siderite		32
Jarosite		8
Marcasite		5
Quartz		3

Experimental setup

Bacterial culture and marine medium

Bacterial culture and medium preparation were carried out following the procedure previously described in Benaiges-Fernández *et al.* (2019) and Palau *et al.* (2021). *Shewanella loihica* was used as a model prokaryote to perform the dissolutive reduction of Fe(III) present in the tailings. *Shewanella* is able to perform bioreduction using Fe(III) and Mn (IV) as a terminal electron acceptor (Gao *et al.*, 1997). Moreover, *Shewanella* is an ubiquitous genus, making it a suitable candidate for the bioreduction experiments. Prior to inoculation into batch and column experiments, *Shewanella* was cultured overnight in LB (Luria-Bertani) medium to attain a late exponential phase of the bacteria. LB medium is a nutrient-rich medium commonly used in microbiological studies. It contains a combination of essential nutrients that support bacterial growth, such as yeast extract, peptone (protein digest), and sodium chloride (Tourney and Ngwenya, 2014). Bacteria were inoculated into the batch and column experiments to reach approximately $1 \cdot 10^7$ ufc mL⁻¹. Inoculation was performed as described in previous works, using a suspension in Ringer ¼ of the bacterial culture grown overnight. The marine medium employed in earlier works (Benaiges-Fernández *et al.*, 2019; Palau *et al.*, 2021) was used in both column and batch experiments. It was amended with sodium lactate (10mM) as an electron donor and carbon source (see the complete composition of the marine medium in Table 2). Before the experiments, the marine medium was sterilized in an autoclave and was bubbled with a constant N₂ flow to remove dissolved oxygen.

Column experiments

Two experiments were conducted using two methacrylate columns of 8cm in diameter and 10cm in length. The columns were sequentially filled from bottom to top with five layers. Each layer was 1.6cm thick with a volume of 0.08dm³. The bottom and top layers were packed with glass beads. The second and fourth layers were composed of acid washed sand, and the third layer was made up of the inoculated tailings samples (CT and PT; Fig. 2A). Controls and replicates were prepared in the same manner.

The porosities estimated from weight/volume ratio and mineral densities of the tailings layers were 60% for CT and 40% for PT. Subsequently, the filled columns were thoroughly saturated with marine medium and allowed to equilibrate overnight. Before initiation of the experiments, the columns were inoculated with bacterial culture and sealed. In order to eliminate oxygen, all procedures were performed inside a glove box filled with N₂. Afterwards, the columns were

TABLE 2. Chemical composition of the marine medium

Component	Concentration (mM)
NaCl	420
Na ₂ SO ₄	30
MgCl ₂ ·6H ₂ O	54
CaCl ₂	10
SrCl ₂ ·6H ₂ O	0.15
KCl	9.32
NaHCO ₃	2.39
KBr	0.84
H ₃ BO ₃	0.43
NaF	0.071
Na lactate	10
TRIS-HCl	10
NH ₄	1.87

extracted from the N₂ glove box and submerged in a cryostatic water bath.

A peristaltic pump was employed to circulate the marine medium through the columns from bottom to top. The flow rates were maintained constant at approximately 0.003mL min⁻¹, yielding residence times of 7.4d and 11.1d in the PT and CT layers, respectively. The columns were immersed in a water bath at constant temperature of 10°C (Fig. 2B). The bath was covered with an opaque lid to guarantee darkness. Column immersion prevented O₂ diffusion through the column wall. A bottle with the input marine medium solution was placed in a glove box purged with N₂ to ensure anoxic conditions (Fig. 2B). In order to prevent O₂ diffusion, stainless steel tubing (0.02m inner diameter) was used to connect the bottles of the input and output solutions with the columns. Both the input and the output solutions were collected from the respective bottles inside the anoxic glove box. The experiments lasted 167days.

Batch experiments

Ten batch experiments were performed using the PT tailings sample following the procedure described in Palau *et al.* (2021). A quarter of a gram (0.25g) of PT tailings was placed in glass vials (25mL; ratio 1:100w/v) filled with marine medium to perform the experiments and the abiotic controls. The experiments were inoculated with the bacterial culture in contrast to the abiotic experiments. Vials were tightly sealed using closed-top screw caps with butyl liner and Parafilm M to minimize headspace and prevent cracking of the tubes from overpressure. The tubes were then stirred for 15s using a vortex mixer and incubated horizontally in a thermostatic water bath at 10±1°C without agitation in

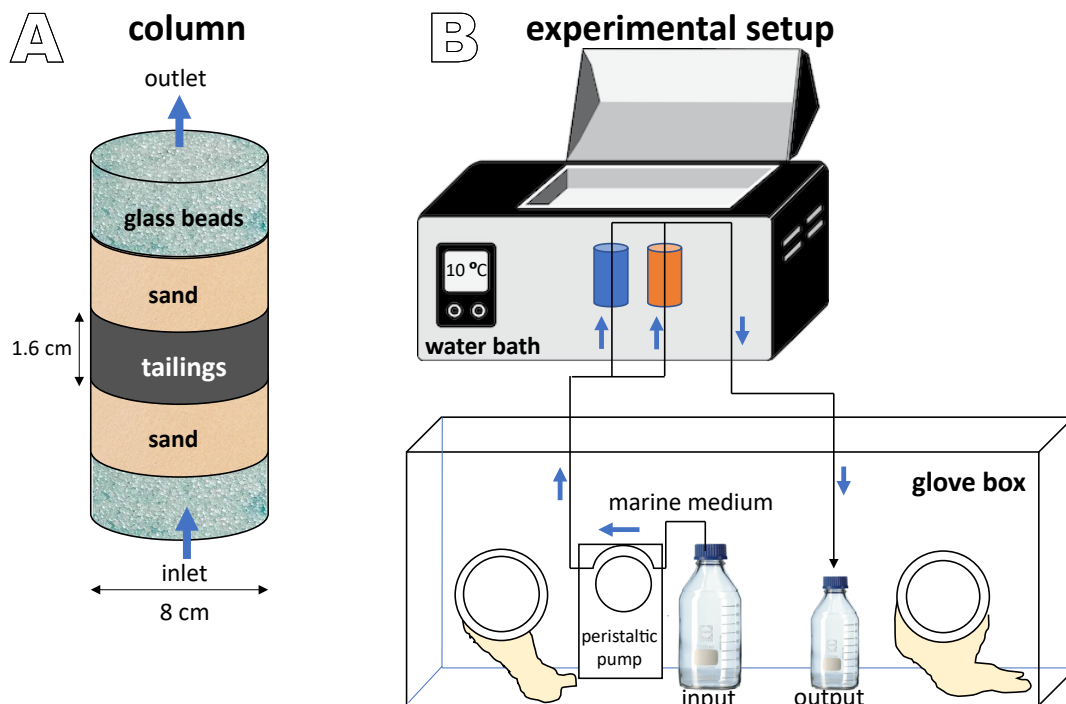


FIGURE 2. Schematic representations of A) a column containing five layers (glass beads, sand and tailings sample) and B) the experimental setup.

the dark for 113 days. Five vials per solid were used in each batch experiment, along with 3 control vials. Vials were sacrificed individually at different time points, following the protocol described by Palau *et al.* (2021). The low incubation temperature and static conditions were chosen to simulate marine sediment environments in standard testing locations. Sampling was performed in a glove box with N_2 atmosphere to maintain the anoxic conditions. Unlike the column experiments, the batch experiments were prepared under atmospheric conditions near a Bunsen burner flame to maintain sterility. *Shewanella loihica* as a facultative anaerobe can use O_2 as a terminal electron acceptor. The rapid consumption of dissolved oxygen in the vials results in anoxic conditions within 24h.

Chemical analysis

Measurements of pH (± 0.02 pH units) and Eh (± 10 mV) were performed using pH and Eh electrodes (Crison and SenTix ORP, Ag/AgCl, WTW, respectively) in the glove box under anoxic conditions. Oxidation-Reduction Potential (ORP) readings were converted to standard Eh values by adding 200 mV to the ORP voltage. At each sampling, the solutions were collected in acid-washed tubes, and two aliquots were taken for analysis. One aliquot was acidified with 100 μ L of fuming HCl to measure lactate and acetate by High Pressure Liquid Chromatography (HPLC). The second aliquot was acidified with 100 μ L of 65% nitric acid to measure the concentrations of minor and major

elements by Inductively Coupled Plasma (ICP) techniques. The aliquots were stored at 4°C until analysis.

Liquid chromatography using a Waters 600 HPLC pump controller equipped with an Aminex HPX-87H column (300 x 7.8 mm), BioRad, and a Waters 717 plus autoinjector was used to measure the concentrations of lactate and acetate. Concentrations of minor elements were analyzed by Inductively Coupled Plasma Mass Spectrometry (ICP-MS) with a Perkin Elmer 350D spectrometer. The analysis of major elements was performed by ICP Optical Emission Spectroscopy (ICP-OES) with a Perkin Elmer Optima 8300 spectrometer equipped with a Charge Injection Device (CID) detector. The uncertainty of the ICP-MS and ICP-OES measurements was $\pm 5\%$. Concentrations of total iron and ferrous iron (Fe(II)) were measured following a modified protocol of the Phenanthroline method (Stucki *et al.*, 1981) with a SP268 830 PLUS, Metertech Inc. spectrophotometer. Triplicate measurements were performed for iron, lactate and acetate (SD is shown in the corresponding plots (Figs. 2-6)).

RESULTS AND DISCUSSION

Tailings composition

In the PT tailings, the predominant minerals are pyrite, siderite and magnetite (Table 1), with high

contents of both Fe(III) and Fe(II). By contrast, the CT tailings contain only 1wt% of magnetite (Table 1), resulting in a significantly lower Fe content. The differences in mineral composition between the two tailings are caused by the concentration processes used in the respective processing plants. At the Ensenada Chapaco plant, although magnetite is the main ore in the Los Colorados mine, most of the profitable iron is in the pellets, leaving a low Fe(III) content in the CT tailings (Knipping *et al.*, n.d.). Moreover, high concentrations of TEs (V, Ti, Mn, Al, Pb and Zn) were detected in the magnetite ore from the Los Colorados deposit (Knipping *et al.*, n.d.).

However, La Unión Mining District La Unión mine had different valuable sources during the years of operation. Changes in mineral extraction for economic reasons (mainly between galena and sphalerite), and the fact that the company was unable to recover magnetite from the tailings, resulted in magnetite-rich tailings. This accounts for the high Fe(II)-Fe(III) content in the PT tailings (Manteca *et al.*, 2014b). Moreover, the magnetite present in the Portman Bay tailings is also rich in TEs such as Pb, Zn, Cu, As and Cd (Gomez-Garcia *et al.*, n.d.; Martínez-Sánchez *et al.*, 2008; Pérez-Sirvent *et al.*, 2018). Overall, these findings underscore the significant influence that the differences in mineral processing exerts on the mineralogical composition of the tailings and their trace element content.

Aqueous chemistry of Portman tailings

Column experiment

The PT and CT column experiments were conducted under an advective flow regime, in which *Shewanella loihica* could catalyze the lactate-acetate oxidation while Fe(III) reduced to Fe(II). In parallel to the column and batch experiments, control experiments were conducted to assess the influence of biotic factors on metal mobilization. Controls showed no significant Fe or TE mobilization, thereby confirming that the trends observed in the main experiments were driven by *Shewanella loihica*. As bioreduction did not occur in the control experiments, these results were not included in the Figures. Note that flat trends related to Fe and TE mobilization in the control experiments are not shown in the plots to avoid confusion.

In the PT column, a high release of Fe (up to 61mM) occurred in the initial 300h (Fig. 3A). Subsequently, the Fe released gradually declined over the course of the experiment. Similar patterns were observed for manganese and zinc with a release of up to 20mM that was followed by a gradual decrease (Fig. 3A). Lactate follows a trend that is similar to that of iron release (Fig. 3B). A high lactate consumption takes place at the outset of the experiment with a consequent release of acetate. Over time, lactate consumption and acetate production drop gradually to concentrations below the detection limit. The initial solution pH of 8.2 decreased to 7.9 during lactate

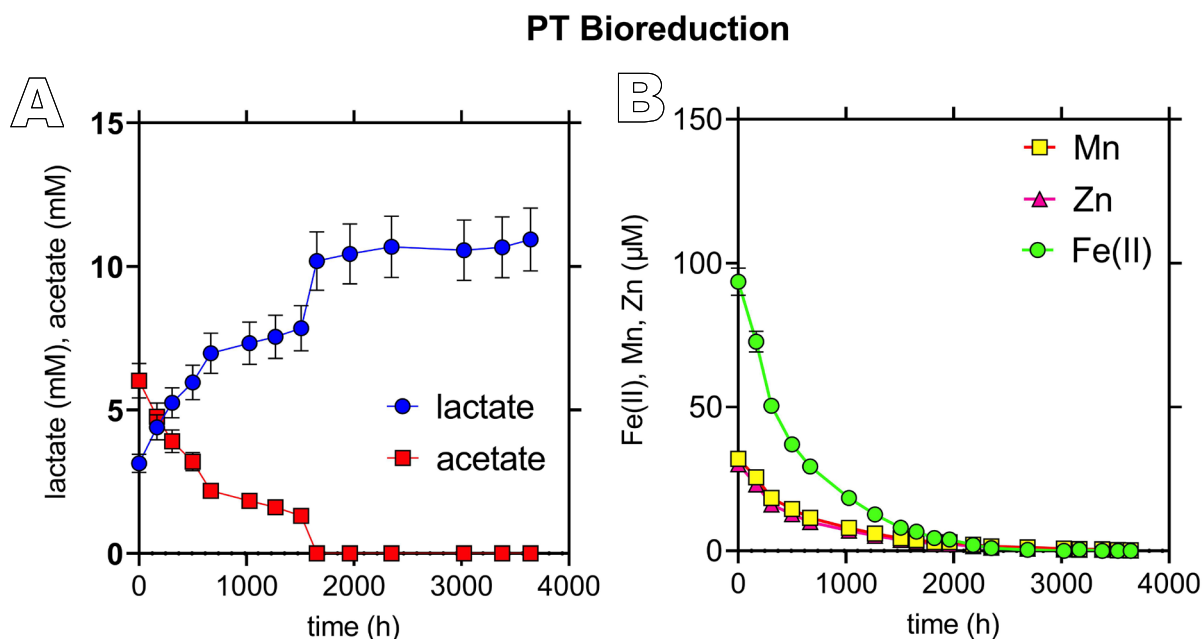


FIGURE 3. Concentration variation diagrams in the PT column. A) lactate and acetate, and B) Fe(II), Zn, and Mn. Error bars represent the standard deviation due to analytical error.

consumption. Thereafter, the pH gradually increased to reach the initial value. The redox potential (Eh) dropped from 200mV to 50-60mV during the experiment.

As for the TE release, the concentrations of Ni, Ti, Pb, V, Cd and Co diminish gradually as does that of Fe(II) (Fig. 4A-G). This variation indicates that the TE release is due to bioreduction, *i.e.* associated with lactate consumption. Cu and Pb are also released (Fig. 4A, D), but the release does not show clear trends throughout the experiment.

The gradual decrease in both the TE and Fe(II) concentrations confirm magnetite bioreduction. A high microbial activity leads to a high magnetite bioreduction that accounts for the elevated TE release in the first hours of the experiment (Figs. 3; 4). A decrease in the activity of *S. loihica* is inferred from a lower lactate consumption that is accompanied by a fall in the concentrations of Fe(II) and TE. Note that in the column experiments, the carbon source is constant because lactate is permanently injected. Therefore, lactate consumption is not the limiting factor in the bioreduction. In contrast, bioreduction halted because of low lactate availability in the batch experiments. The cessation of microbial activity observed after 2000h is due to the low Fe(III) bioavailability in the tailings. This is because the Fe(II) released during magnetite bioreduction is partially adsorbed onto the magnetite surface as suggested in (Benaiges-Fernández *et al.*, 2019; Boland *et al.*, 2014; Palau *et al.*, 2021).

Batch experiments

In the batch experiments, bioreduction of the PT tailings also occurred under marine conditions as shown in earlier studies (Benaiges-Fernández *et al.*, 2019; Palau *et al.*, 2021). At the start of the experiment, a large manganese concentration is released before iron (Fig. 5A). This indicates that the Mn(IV) associated with magnetite and Mn-oxides in the tailings (Frietsch, 1982; Lu *et al.*, 1994) can also be bioreduced to Mn(II) and Mn(III) and that *Shewanella loihica* prefers Mn to Fe (Gao *et al.*, 1997). Similar trends in the release of Mn were observed in magnetite with high contents of Mn (Benaiges-Fernández *et al.*, 2019). Nevertheless, an initial Fe(II) adsorption onto magnetite cannot be ruled out (Gorski *et al.*, 2011). The Fe(II) release occurred after 50 d when most of the Mn was reduced (Fig. 5A). Remarkably, the quantities of Fe(II) released in the batch experiments are similar to those in the column experiments (1.2mmol and 1.3mmol Fe(II) g tailing⁻¹, respectively). A simultaneous release of Al, Zn, As and TEs (Cu, V, Ni, Pb and Ti) occurs throughout the experiment (Fig. 5B, C).

Aqueous chemistry of Los Colorados Tailings

In the CT column, a roughly constant Fe release ($[Fe] \approx 10 \mu\text{M}$) occurs during the experimental run (Fig. 6B). The Mn and Zn release exhibits a pattern similar to Fe(II), *i.e.* fairly constant ($[Zn] = 20 \mu\text{M}$; Fig. 6B), although a gradual

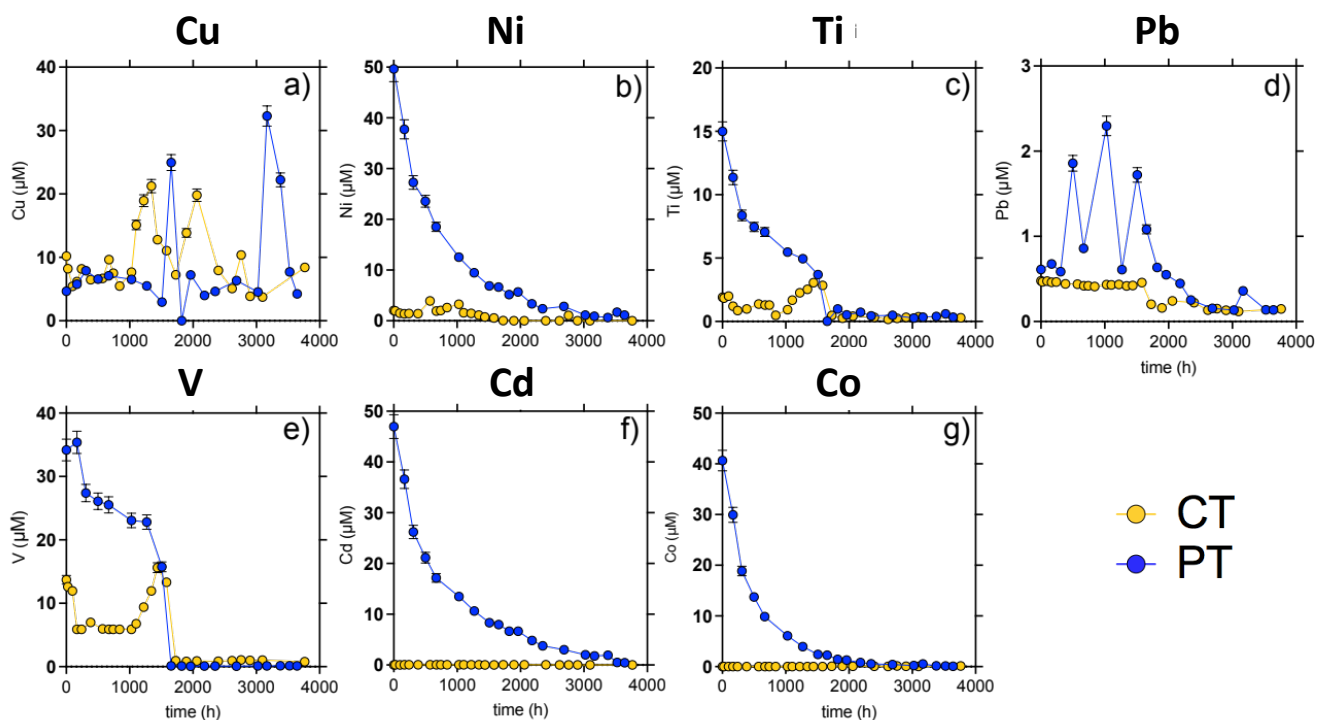


FIGURE 4. Variation in trace element concentrations over time in the PT and CT columns. A) Copper. B) Nickel. C) Titanium. D) Lead. E) Vanadium. F) Cadmium. G) Cobalt. Error bars represent the standard deviation due to analytical error.

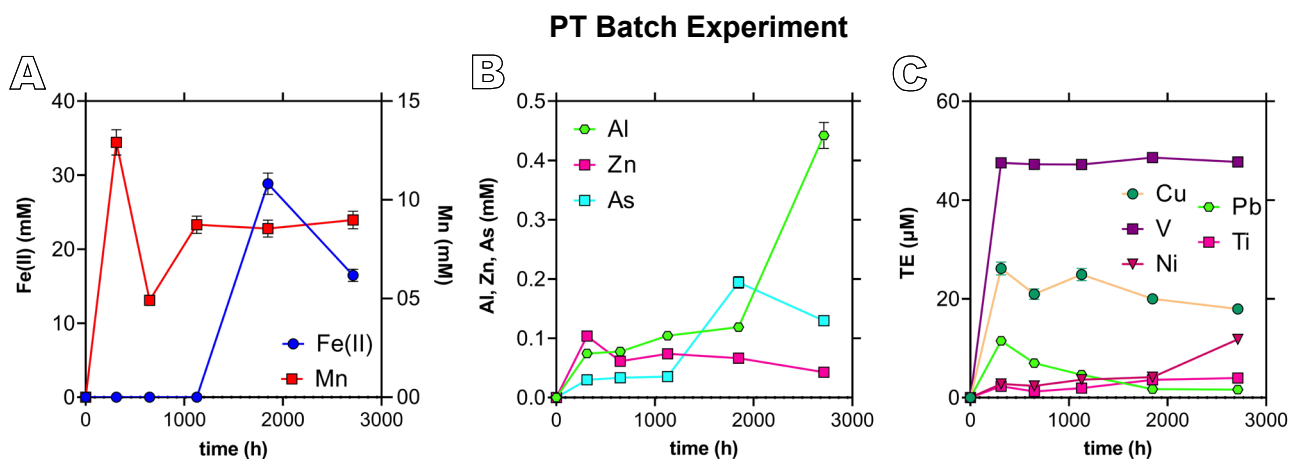


FIGURE 5. Variation plots of element concentration in the batch experiment with Portman tailings. A) Fe(II) and Mn. B) trace elements (Al, Zn, and As). Error bars represent the standard deviation due to analytical error.

potential (Eh) gradually drops from 150-200mV to 50mV during the experiment. Eh values of ≈ 50 mV indicate an oxide-reduction level that is comparable to the one observed in iron reduction in sea sediment (Lovley and Phillips, 1986).

During the experiment, Cu concentration fluctuates between $4\mu\text{M}$ and $22\mu\text{M}$ (Fig. 4A). The concentration trends of Ni, Ti, and Cd (Fig. 4B, C, F) are similar to that of Zn (Fig. 6B). Pb concentration is high during the first half of the experiment (~ 2000 h) and is followed by a gradual decline (Fig. 4D). V concentration increases in the first 165h (Fig. 4E) and drops before remaining constant for the next 800h. Finally, it increases and stabilizes until the end of the experiment. Overall, the TE release across the two

lower in the CT tailings (5.4mmol) than in the PT tailings (168.3mmol). The magnitude of bioreduction is therefore expected to be higher in the PT column as indicates the longer production of acetate in the CT tailings (Figs. 3A; 6B).

In the PT column, after normalizing the release of bioreduced Fe(II) to the initial content of Fe(III) in the tailings sample, 95% of Fe(III) is consumed after 2000h (Fig. 3B). At this point, the low microbial activity is dependent on the low Fe(III) concentration. By contrast, the bioreduced Fe(III) is 8% in the CT column. The decrease in microbial activity is due to the low thermodynamic efficiency of *S. loihica* when using Fe(III) in the CT tailings as a Terminal Electron Acceptor (TEA). Thus, as shown in

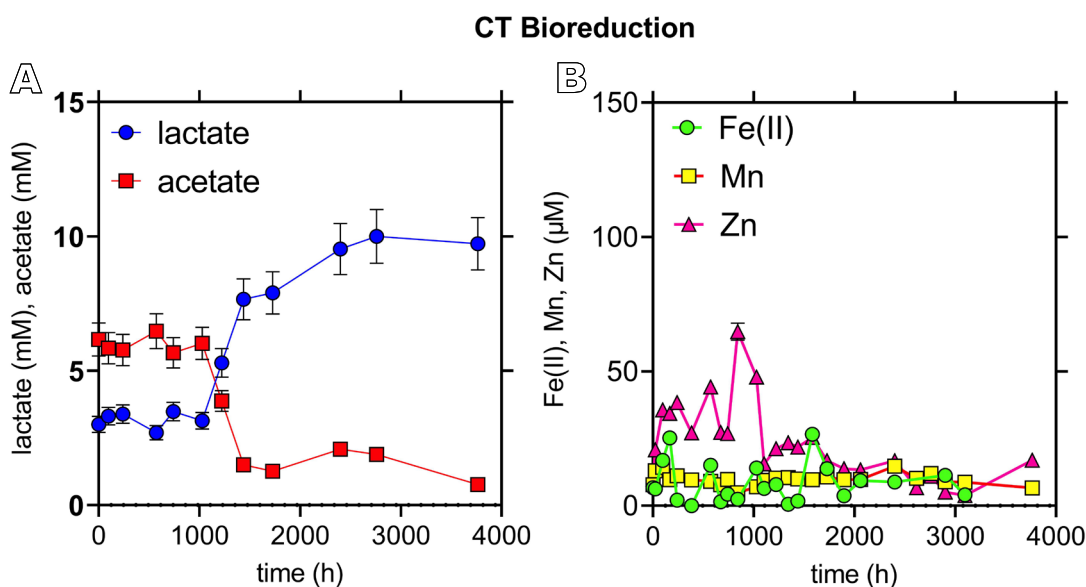


FIGURE 6. Concentration variation diagrams in the CT column. A) Lactate and acetate. B) Fe(II), Mn, and Zn. Error bars represent the standard deviation due to analytical error.

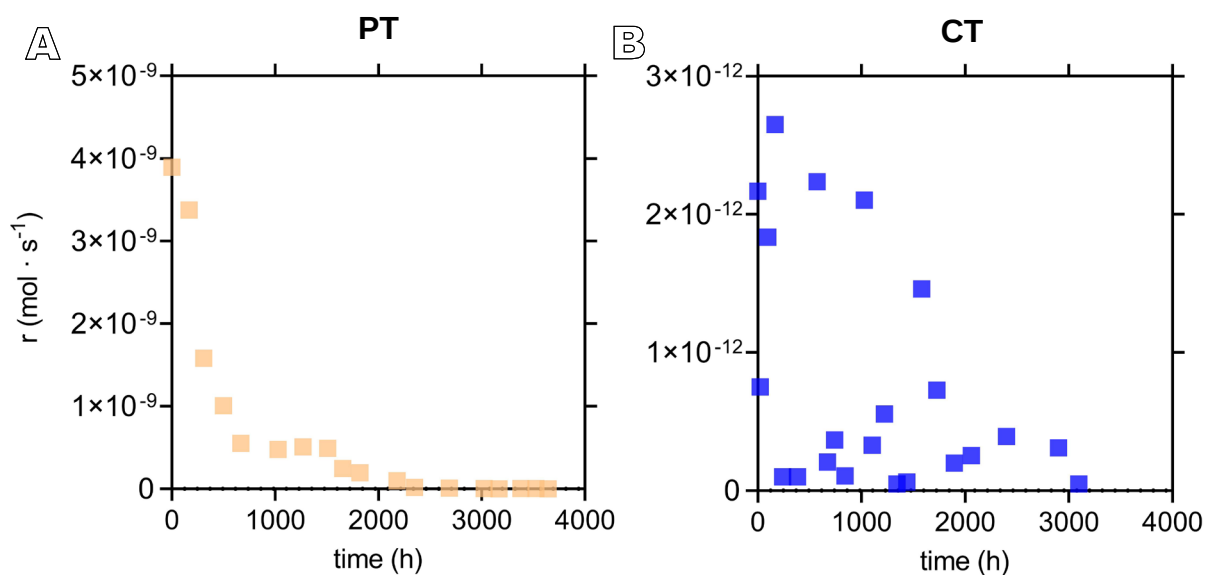


FIGURE 7. Bioreduction rate ($\text{mol} \cdot \text{s}^{-1}$) variation plots. A) PT column. B) CT column.

previous studies (Palau *et al.*, 2021), *S. loihica* is unable to maintain a sufficient bacterial population using a low profit TEA, limiting the Fe(III) bioreduction (Liu *et al.*, 2001a, b; Urrutia *et al.*, 1998).

A key parameter in bioreduction kinetics is the reactive surface area of the iron (hydr)oxide involved in the reaction (Benaiges-Fernandez *et al.*, 2019; Palau *et al.*, 2021). A larger surface area provides more bacterial attachment, increasing thus the bioreduction rate. Additionally, Dippon *et al.* (2015) showed that biogenic iron mineral transformation depends on the kinetic properties of the reaction system (*e.g.* chemical and biological dissolution kinetics and the presence of catalysts). Given the lower magnetite content in the CT tailings sample, there is less magnetite surface area for *S. loihica* to attach and bioreduce (El-Naggar *et al.*, 2010). Consequently, a low reactive surface area diminishes bioreduction in the CT column. By contrast, the magnetite content in the PT column is higher than in the CT column, yielding a larger magnetite reactive surface area (*i.e.* a higher bioreduction rate).

In the column experiments, lactate is permanently supplied, unlike in the batch experiments, where the ratio between lactate and available Fe(III) is lower than that in the columns. As a result, magnetite bioreduction is controlled by Fe(III) rather than by substrate (*i.e.* lactate), where the availability of Fe(III) is proportional to the magnetite reactive surface area. Average bioreduction rates (r in $\text{mol} \cdot \text{s}^{-1}$) in the columns were calculated using the experimental flow rate (Q in $\text{L} \cdot \text{s}^{-1}$) and the measured aqueous Fe(II) concentration of the output solutions ($C_{\text{Fe(II)}}$ in $\text{mol} \cdot \text{L}^{-1}$;

$R = Q \cdot C$; Fig. 7). Since the column with the PT tailings has a higher Fe(III) content and a larger magnetite surface area, the initial bioreduction rate is higher in the PT column ($\approx 3.4 \cdot 10^{-9} \text{ mol} \cdot \text{s}^{-1}$) than in the CT column ($2.2 \cdot 10^{-12} \text{ mol} \cdot \text{s}^{-1}$; Fig. 7A, B).

In the PT column, the larger magnetite surface area results in a higher bioreduction rate, initially causing a significant release of Fe(II) (Fig. 3B). However, this release is only a portion of the total Fe(III) bioreduced, as Fe(II) is mostly adsorbed onto the solid phase. Over time, Fe(II) adsorbs onto the magnetite surface, decreasing the available reactive surface area. As a consequence, Fe(III) accessible to bacteria declines, diminishing the bioreduction rate (Fig. 7A).

In the CT column, the bioreduction rate remains roughly constant for 1000h (Fig. 7B) as inferred from the Fe(II) concentrations (Fig. 6B). Thereafter, the rate drops in the following 1500h until the cessation of bioreduction after 2500h (Fig. 7B). However, as the initial release of Fe(II) in the CT column is lower than in the PT column, the effect of Fe(II) adsorption on the bioreduction rate is smaller. In such a case, as Fe(II) adsorption is slow, the availability of Fe(III) for reduction by bacteria lasts longer.

Similar trends of bioreduction of Fe and TE mobilization (*e.g.* Mn, Ni and Pb) were observed in the CT and PT columns, as well as a similar preference for Mn as an electron acceptor by *Shewanella loihica*. A larger content and surface area of magnetite in the PT column led to a higher initial rate of bioreduction with more Fe(II). Over time, adsorption of Fe(II) to magnetite diminished

the available reactive surface area. This led to a decrease in Fe(III) for reduction and to a subsequent the rate of bioreduction (Fig. 7A).

Bioreduction in the CT column took place at a much slower rate and at a more linear rate. Taking into account the lower initial concentration of Fe(III) and the smaller reactive surface area of magnetite, the rate of Fe(II) generation diminished. Hence, the effect of Fe(II) adsorption on the rate of bioreduction was not critical, and Fe(III) reduction lasted longer than in the PT column.

Trends in the release of Ni and Pb were similar in both column experiments, although maximum concentrations differed because the contents of magnetite and the behavior of Fe(II) were distinct. The initial Mn depletion, and the subsequent Fe bioreduction and trace element mobilization indicate a strong interdependence between the mineralogical properties (e.g. reactive surface area and Fe²⁺/Fe³⁺ availability), the bioreduction processes, and the subsequent release of trace elements.

CONCLUSIONS

The column and batch experiments performed with the Portman Bay and Ensenada Chapaco tailings confirm the magnetite bioreduction under marine conditions (i.e. O₂-free atmosphere and 10°C in the dark).

With sufficient lactate (i.e. organic matter), magnetite bioreduction depends on the availability of Fe(III), which in turn depends on the content and reactive surface area of magnetite. As Fe(II) adsorbs onto magnetite inducing the formation of a secondary magnetite, the reactive surface area diminishes, limiting the availability of Fe(III) and lowering the bioreduction rate.

The variation in the bioreduction rates calculated as a function of time and Fe(II) concentration is of importance for the management of Submarine Tailings Disposal (STD). It is shown that the bioreduction rate is affected by the decrease in the reactive surface area, which is caused by Fe(II) adsorption onto magnetite.

The concentrations of TE (e.g. vanadium, copper, nickel, cobalt, titanium, lead and cadmium) released in the experiments exceed those found under natural marine conditions. The overall process, therefore, suggests that an uninterrupted disposal of iron-oxide STD results in a permanent bioreduction of tailings with the consequent metal release whenever Fe(III) is available. A metal contamination and accumulation in the flora and fauna of the sea would pose a great risk to the environment.

ACKNOWLEDGMENTS

We would like to thank Natàlia Moreno, Rafael Bartolí and Mercè Cabanas (IDAEA), David Artiga, Maite Romero and Xavier LLOvet (SCT-Barcelona University) for analytical assistance. This work has been financed by the CGL2017-82331-R (Spanish Ministry of Economy and Competitiveness) and PID2020-119196RB-C22 (Spanish Ministry of Science and Innovation) projects, the 2021 SGR 00308 project (Catalan Government) and the Chilean Government through the Research Fund for Fishery and Aquaculture (Fondo de Investigación Pesquera y de Acuicultura; FIPA) of SUBPESCA (FIP 2015-11 project). IDAEA-CSIC is a Severo Ochoa Center of Excellence (Spanish Ministry of Science and Innovation, Project CEX2018-000794-S funded by MCIN/AEI/10.13039/501100011033).

REFERENCES

- Alorda-Kleinglass, A., Garcia-Orellana, J., Rodellas, V., Cerdà-Domènech, M., Tovar-Sánchez, A., Diego-Feliu, M., Trezzi, G., Sánchez-Quilez, D., Sanchez-Vidal, A., Canals, M., 2019. Remobilization of dissolved metals from a coastal mine tailing deposit driven by groundwater discharge and porewater exchange. *Science of The Total Environment*, 688, 1359-1372. DOI: <https://doi.org/10.1016/J.SCITOTENV.2019.06.224>
- Autónoma De Baja, U., México Benedicto, C., Martínez-Gómez, J., Guerrero, C., Jornet, J., Rodríguez, A., 2008. Ciencias Marinas Metal contamination in Portman Bay (Murcia, SE Spain) 15 years after the cessation of mining activities. *Cienc Mar*, 34, 389-398.
- Benaiges-Fernandez, R., Palau, J., Offeddu, FG., Cama, J., Urmeneta, J., Soler, J.M., Dold, B., 2019. Dissimilatory bioreduction of iron (III) oxides by *Shewanella loihica* under marine sediment conditions. *Mar Environ Res*, 151, 104782. DOI: <https://doi.org/10.1016/J.MARENRES.2019.104782>
- Benavente, D., Pla, C., Valdes-Abellan, J., Cremades-Altred, S., 2020. Remediation by waste marble powder and lime of jarosite-rich sediments from Portman Bay (Spain). *Environmental Pollution*, 264. DOI: <https://doi.org/10.1016/J.ENVPOL.2020.114786>
- Boland, D.D., Collins, R.N., Miller, C.J., Glover, C.J., David Waite, T., 2014. Effect of solution and solid-phase conditions on the Fe (II)-accelerated transformation of ferrihydrite to lepidocrocite and goethite. *ACS Publications*, 48, 15. DOI: <https://doi.org/10.1021/es4043275>
- Chen, Z., Wang, Y., Xia, D., Jiang, X., Fu, D., Shen, L., Wang, H., Li, Q.B., 2016. Enhanced bioreduction of iron and arsenic in sediment by biochar amendment influencing microbial community composition and dissolved organic matter content and composition. *J Hazard Mater*, 311, 20-29. DOI: <https://doi.org/10.1016/J.JHAZMAT.2016.02.069>
- Davies, E., science, R.N.-R. studies in marine, 2017, undefined, n.d. In situ characterisation of complex suspended particulates surrounding an active submarine tailings placement site in a Norwegian fjord. Elsevier.

- 1 Dippon, U., Schmidt, C., Behrens, S., Kappler, A., 2015. Secondary
2 Mineral Formation During Ferrihydrite Reduction by
3 *Shewanella oneidensis* MR-1 Depends on Incubation Vessel
4 Orientation and Resulting Gradients of Cells, Fe²⁺ and Fe
5 Minerals. *Geomicrobiol J*, 32, 878-889. DOI: [https://doi.org/](https://doi.org/10.1080/01490451.2015.1017623)
6 [10.1080/01490451.2015.1017623](https://doi.org/10.1080/01490451.2015.1017623)
- 7 Dold, B., 2014. Submarine Tailings Disposal (STD)—A
8 Review. *Minerals*, 4, 642-666. DOI: <https://doi.org/10.3390/>
9 [MIN4030642](https://doi.org/10.3390/MIN4030642)
- 10 dos Santos, R.W., Schmidt, É.C., de L Felix, M.R., Polo, L.K.,
11 Kreuzsch, M., Pereira, D.T., Costa, G.B., Simioni, C., Chow, F.,
12 Ramlov, F., Maraschin, M., Bouzon, Z.L., 2014. Bioabsorption
13 of cadmium, copper and lead by the red macroalga *Gelidium*
14 *floridanum*: Physiological responses and ultrastructure
15 features. *Ecotoxicol Environ Saf*, 105, 80-89. DOI: [https://doi.org/](https://doi.org/10.1016/J.ECOENV.2014.02.021)
16 [10.1016/J.ECOENV.2014.02.021](https://doi.org/10.1016/J.ECOENV.2014.02.021)
- 17 El-Naggar, M.Y., Wanger, G., Leung, K.M., Yuzvinsky, T.D.,
18 Southam, G., Yang, J., Lau, W.M., Neelson, K.H., Gorby,
19 Y.A., 2010. Electrical transport along bacterial nanowires
20 from *Shewanella oneidensis* MR-1. *Proc Natl Acad Sci*
21 *U S A*, 107, 18127-18131. DOI: <https://doi.org/10.1073/>
22 [PNAS.1004880107](https://doi.org/10.1073/PNAS.1004880107)
- 23 Esther, J., Sukla, L.B., Pradhan, N., Panda, S., 2015. Fe (III)
24 reduction strategies of dissimilatory iron reducing bacteria.
25 *Korean Journal of Chemical Engineering*, 32, 1-14. DOI:
26 <https://doi.org/10.1007/S11814-014-0286-X>
- 27 Frietsch, R., 1982. Chemical composition of magnetite
28 and sphalerite in the iron and sulphide ores of
29 central sweden. *GFF* 104, 43-47. DOI: [https://doi.org/](https://doi.org/10.1080/11035898209454534)
30 [10.1080/11035898209454534](https://doi.org/10.1080/11035898209454534)
- 31 Gao, H., Obratova, A., Stewart, N., Popa, R., Fredrickson, J.K.,
32 Tiedje, J.M., Neelson, K.H., Zhou, J., 1997. *Shewanella*
33 *loihica* sp. nov., isolated from iron-rich microbial mats in
34 the Pacific Ocean. *International Journal of Systematic and*
35 *Evolutionary Microbiology*, 56, 1911-1916. DOI: [https://doi.org/](https://doi.org/10.1099/ijs.0.64354-0)
36 [10.1099/ijs.0.64354-0](https://doi.org/10.1099/ijs.0.64354-0)
- 37 Gomez-Garcia, C., ... F.M.-H.-J. of A., 2015, undefined, n.d. Rock
38 magnetic characterization of the mine tailings in Portman Bay
39 (Murcia, Spain) and its contribution to the understanding of
40 the bay infilling process. Elsevier.
- 41 González, S.A., Stotz, W., Lancellotti, D., 2014. Effects of the
42 discharge of iron ore tailings on subtidal rocky-bottom
43 communities in northern Chile. *Journal of Coastal*
44 *Research*, 30(3), 500-514. DOI: <https://doi.org/10.2112/>
45 [JCOASTRES-D-12-00086.1](https://doi.org/10.2112/JCOASTRES-D-12-00086.1)
- 46 Gorski, C., Chemistry, M.S.-A.R., 2011, undefined. Fe²⁺ Sorption
47 at the Fe Oxide-Water Interface: A Revised Conceptual
48 Framework. ACS Publications, 1071, 315-343. DOI: [https://](https://doi.org/10.1021/bk-2011-1071.ch015)
49 doi.org/10.1021/bk-2011-1071.ch015
- 50 Jensen, T., assessment, K.H.-I. environmental, 2019, undefined,
51 2019. Environmental adaptive management: application on
52 submarine mine tailings disposal. Wiley Online Library, 15,
53 575-583. DOI: <https://doi.org/10.1002/ieam.4134>
- 54 Knipping, J., Bilenker, L., Simon, A., Acta, M.R.-... et C., 2015,
55 undefined, n.d. Trace elements in magnetite from massive
iron oxide-apatite deposits indicate a combined formation by
igneous and magmatic-hydrothermal processes. Elsevier.
- Koski, R.A., 2012. Metal dispersion resulting from mining
activities in coastal environments: A pathways approach.
Oceanography, 25, 170-183. DOI: <https://doi.org/10.5670/>
OCEANO.2012.53
- Kwong, Y.T.J., Apte, S.C., Asmund, G., Haywood, M.D.E., Morello,
E.B., 2019. Comparison of Environmental Impacts of Deep-
sea Tailings Placement Versus On-land Disposal. *Water Air*
Soil Pollut, 230. DOI: <https://doi.org/10.1007/S11270-019->
4336-1
- Lancellotti, D., Bulletin, W.S.-M.P., 2004, undefined, n.d. Effects
of shoreline discharge of iron mine tailings on a marine soft-
bottom community in northern Chile. Elsevier.
- Liu, C., Kota, S., Zachara, J., ... J.F.-E., undefined, 2001a.
Kinetic analysis of the bacterial reduction of goethite. ACS
Publications, 35, 2482-2490. DOI: <https://doi.org/10.1021/>
es001956c
- Liu, C., Zachara, J., technology, Y.G.-... science &, undefined,
2001b. Microbial Reduction of Fe(III) and Sorption/
Precipitation of Fe(II) on *Shewanella putrefaciens* Strain
CN32. ACS Publications, 35, 1385-1393. DOI: [https://doi.org/](https://doi.org/10.1021/es0015139)
10.1021/es0015139
- Lonergan, D.J., Jenter, H.L., Coates, J.D., Phillips, E.J.P., Schmidt,
T.M., Lovley, D.R., 1996. Phylogenetic analysis of dissimilatory
Fe(III)-reducing bacteria. *J Bacteriol*, 178, 2402-2408. DOI:
<https://doi.org/10.1128/JB.178.8.2402-2408.1996>
- Lovley, D.R., Phillips, E.J.P., 1986. Organic Matter Mineralization
with Reduction of Ferric Iron in Anaerobic Sediments.
Appl Environ Microbiol, 51, 683-689. DOI: [https://doi.org/](https://doi.org/10.1128/AEM.51.4.683-689.1986)
10.1128/AEM.51.4.683-689.1986
- Lu, R., Solid, S.B.-J. of G.R., undefined, 1994. Magnetite
dissolution in deep sediments and its hydrologic implication:
a detailed study of sediments from site 808, leg 131.
Wiley Online Library, 99, 9051-9059. DOI: [https://doi.org/](https://doi.org/10.1029/93JB03204)
10.1029/93JB03204
- Manteca, J.I., García, J.Á.L., Oyarzun, R., Carmona, C., 2014a.
The beach placer iron deposit of Portman Bay, Murcia, SE
Spain: The result of 33 years of tailings disposal (1957–1990)
to the Mediterranean seaside. *Miner Depos*, 49, 777-783.
DOI: <https://doi.org/10.1007/S00126-014-0511-X>
- Manteca, J.I., García, J.Á.L., Oyarzun, R., Carmona, C., 2014b.
The beach placer iron deposit of Portman Bay, Murcia, SE
Spain: The result of 33 years of tailings disposal (1957–1990)
to the Mediterranean seaside. *Miner Depos*, 49, 777-783.
<https://doi.org/10.1007/S00126-014-0511-X>
- Martínez-Sánchez, M.J., Navarro, M.C., Pérez-Sirvent, C.,
Marimón, J., Vidal, J., García-Lorenzo, M.L., Bech, J., 2008.
Assessment of the mobility of metals in a mining-impacted
coastal area (Spain, Western Mediterranean). *J Geochem*
Explor, 96, 171-182. DOI: [https://doi.org/10.1016/J.](https://doi.org/10.1016/J.GEXPLO.2007.04.006)
GEXPLO.2007.04.006
- Medina, M., Andrade, S., Faugeron, S., Lagos, N., Mella, D.,
Correa, J.A., 2005. Biodiversity of rocky intertidal benthic
communities associated with copper mine tailing discharges

- 1 in northern Chile. *Mar Pollut Bull*, 50, 396-409. DOI: <https://doi.org/10.1016/J.MARPOLBUL.2004.11.022>
- 2
- 3 Palau, J., Benaiges-Fernandez, R., Offeddu, F., Urmeneta, J., Soler, J.M., Cama, J., Dold, B., 2021. Release of trace elements during bioreductive dissolution of magnetite from metal mine tailings: Potential impact on marine environments. *Science of The Total Environment*, 788, 147579. DOI: <https://doi.org/10.1016/J.SCITOTENV.2021.147579>
- 4
- 5
- 6
- 7
- 8
- 9 Peña, J., Manteca, J., ... P.M.-P.-J. of A., 2013, undefined, n.d. Magnetic gradient map of the mine tailings in Portman Bay (Murcia, Spain) and its contribution to the understanding of the bay infilling process. Elsevier.
- 10
- 11
- 12
- 13 Pérez-Sirvent, C., García-Lorenzo, M.L., Hernández-Pérez, C., Martínez-Sánchez, M.J., 2018. Assessment of potentially toxic element contamination in soils from Portman Bay (SE, Spain). *J Soils Sediments*, 18, 2248-2258. DOI: <https://doi.org/10.1007/S11368-017-1756-7/FIGURES/4>
- 14
- 15
- 16
- 17
- 18 Proceeding of the GESAMP International Workshop on the Impacts of Mine Tailings in the Marine Environment | GESAMP [WWW Document], n.d. URL <http://www.gesamp.org/publications/workshop-on-impacts-of-mine-tailings> (accessed 3.23.23).
- 19
- 20
- 21
- 22
- 23 Rahfeld, A., Kleeberg, R., Möckel, R., Gutzmer, J., 2018. Quantitative mineralogical analysis of European Kupferschiefer ore. *Miner Eng*, 115, 21-32. DOI: <https://doi.org/10.1016/J.MINENG.2017.10.007>
- 24
- 25
- 26
- 27 Ramirez-Llodra, E., Trannum, H., ... G.A.-M.P., 2022, undefined, n.d. New insights into submarine tailing disposal for a reduced environmental footprint: Lessons learnt from Norwegian fjords. Elsevier.
- 28
- 29
- 30
- 31 Ramirez-Llodra, E., Trannum, H.C., Evenset, A., Levin, L.A., Andersson, M., Finne, T.E., Hilario, A., Flem, B., Christensen, G., Schaanning, M., Vanreusel, A., 2015. Submarine and deep-sea mine tailing placements: A review of current practices, environmental issues, natural analogs and knowledge gaps in Norway and internationally. *Mar Pollut Bull*. DOI: <https://doi.org/10.1016/j.marpolbul.2015.05.062>
- 32
- 33
- 34
- 35
- 36
- 37
- 38 Sillitoe, R.H., 2003. Iron oxide-copper-gold deposits: An Andean view. *Miner Depos*, 38, 787-812. DOI: <https://doi.org/10.1007/S00126-003-0379-7/METRICS>
- 39
- 40
- 41
- 42
- 43
- 44
- 45
- 46
- 47
- 48
- 49
- 50
- 51
- 52
- 53
- 54
- 55

Manuscript received February 2024;
revision accepted January 2025;
published Online February 2025.